3 Quantum Dynamics of Molecules

3.1 Born-Oppenheimer approximation

The Born-Oppenheimer approximation has been introduced in previous lectures. Briefly, we write the full molecular Hamiltonian in Cartesian coordinates:

$$\begin{aligned}\hat{H} &= \sum_i -\frac{\hbar^2\nabla_{e,i}^2}{2m_e} + \sum_i -\frac{\hbar^2\nabla_{N,i}^2}{2M_i} + \frac{1}{4\pi\epsilon_0}\left(\sum_{j>i}\frac{e^2}{|\vec{r_i}-\vec{r_j}|} + \sum_{j>i}\frac{Z_iZ_je^2}{|\vec{R_i}-\vec{R_j}|} - \sum_{i,j}\frac{Z_je^2}{|\vec{r_i}-\vec{R_j}|}\right) \\ &\equiv \hat{T}_e + \hat{T}_N + \hat{V}_e + \hat{V}_N + \hat{V}_{eN}\end{aligned} \tag{3.1}$$

- $\{\vec{r}, \nabla_e\}, m_e$ refers to electrons.
- $\{\vec{R}, \nabla_N\}, M_i$ refers to nuclei.

The TISE in the full coordinate space of nuclei and electrons is

$$\hat{H}(\vec{r},\vec{R})\Psi(\vec{r},\vec{R}) = E\Psi(\vec{r},\vec{R}). \tag{3.2}$$

We find an approximate solution by fixing $\vec{R}$ and solving an electronic TISE:

$$\begin{aligned}\hat{H}_e\varphi(\vec{r};\vec{R}) &= E(\vec{R})\varphi(\vec{r};\vec{R}), \\ \text{where} \qquad \hat{H}_e &= \hat{T}_e + \hat{V}_e + \hat{V}_{eN}.\end{aligned} \tag{3.3}$$

We assume that the full molecular wavefunction (adiabatic wavefunction) can be written as a product

$$\Psi(\vec{r},\vec{R}) = \varphi(\vec{r};\vec{R})\chi(\vec{R}). \tag{3.4}$$

Substituting this ansatz into full TISE equation (3.2) we obtain

$$\begin{aligned}\hat{H}(\vec{r},\vec{R})[\varphi(\vec{r};\vec{R})\chi(\vec{R})] = [E(\vec{R}) + \hat{V}_N]\varphi(\vec{r};\vec{R})\chi(\vec{R}) + \\ \sum_i -\frac{\hbar^2}{2M_i}\left[\varphi(\vec{r};\vec{R})\nabla^2\chi(\vec{R}) + 2\nabla\varphi(\vec{r};\vec{R})\cdot\nabla\chi(\vec{R}) + \nabla^2\varphi(\vec{r};\vec{R})\chi(\vec{R})\right] \\ = E\varphi(\vec{r};\vec{R})\chi(\vec{R}),\end{aligned} \tag{3.5}$$

where ∇ is used to represent ∇_N.

The last two terms are proportional to m_e/M_N to some power and are therefore several orders of magnitude smaller than the other terms. Neglecting them yields

$$\begin{aligned}\hat{H}(\vec{r},\vec{R})\chi(\vec{R}) &= [\hat{T}_N + E(\vec{R}) + \hat{V}_N(\vec{R})]\chi(\vec{R}) \\ &= E\chi(\vec{R}),\end{aligned} \tag{3.6}$$

which is a TISE for nuclei under an adiabatic Hamiltonian whose effective potential is $E(\vec{R})+V_N(\vec{R})$. The set of approximations leading to equation (3.6) are known as the Born-Oppenheimer approximation.

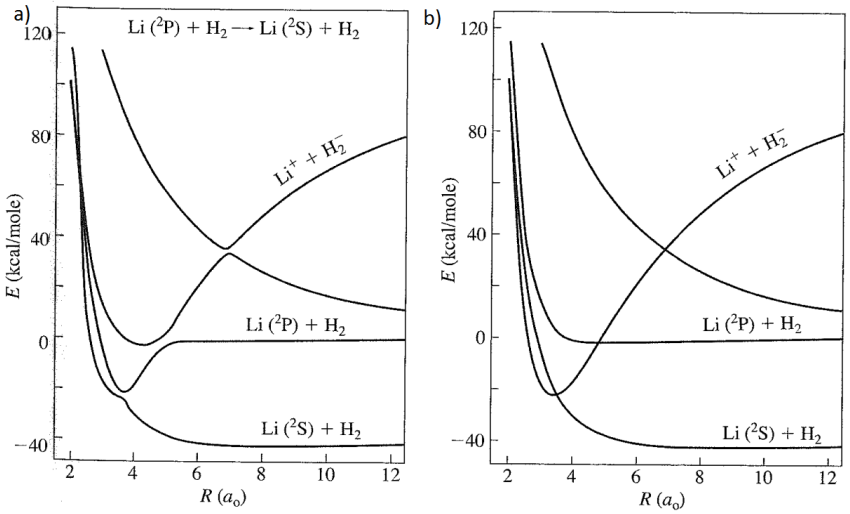

Figure 3.1: Slices of the four lowest potential energy surfaces of a particular symmetry of LiH_2 as a function of the Li-H_2 separation. The orientation of the H_2 internuclear axis is 60° relative to the Li-H_2 direction, and the H_2 internuclear distance is 1.4 Å (adiabatic representation). Note that the adiabatic potentials, being of the same symmetry, obey a "non-crossing" rule. At the avoided crossings, the physical characters of the adiabatic electronic states generally change, for example, from ionic to covalent. (b) Diabatic representation, potentials have continuous physical character. (taken from Introduction to quantum mechanics, David J. Tannor)

3.2 Adiabatic and diabatic representation

The description of molecular dynamics in electronically excited states almost systematically requires a description beyond the Born-Oppenheimer approximation. Such descriptions can be made either in the (unique) adiabatic representation or in one (of infinitely many) diabatic representations. The ensemble of electronic states of any of these representations forms a complete basis.

3.2.1 Adiabatic representation

It is possible to go beyond the Born-Oppenheimer approximation by writing a formally exact solution[1]

$$\psi(\vec{r};\vec{R}) = \sum_{n=0}^{\infty} \varphi_n(\vec{r};\vec{R})\chi_n(\vec{R}). \tag{3.7}$$

Substituting this ansatz equation (3.7) into equation (3.5), multiplying from the left with $\varphi_m(\vec{r};\vec{R})$ and integrating over the electronic coordinates yields a set of coupled equations:

$$\begin{aligned}
\sum_n H_{mn}(\vec{R})\chi_n(\vec{R}) &= \sum_n \left\{ \left[\hat{T}_N + E_n(\vec{R}) + \hat{V}_N(\vec{R})\right]\delta_{mn} + 2T^{(1)}_{mn}(\vec{R})\cdot\nabla + T^{(2)}_{mn}(\vec{R}) \right\} \chi_n(\vec{R}) \\
&= E\chi_m(\vec{R}) \\
\text{where} \quad T^{(1)}_{mn}(\vec{R}) &= \langle\varphi_m|\nabla\varphi_n\rangle \\
\text{and} \quad T^{(2)}_{mn}(\vec{R}) &= \langle\varphi_m|\nabla^2\varphi_n\rangle
\end{aligned} \tag{3.8}$$

with Dirac brakets referring only to integration over electronic coordinates. ∇ is a symbol for the multi-dimensional derivative with respect to mass-weighted nuclear coordinates, $T^{(1)}_{mn}$ is a vector with a number of components equal to the number of vibrational degrees of freedom; $T^{(2)}_{mn}$ is a scalar. Taking the electronic wave functions as normlized to the same value at all nuclear geometries $\langle\varphi_m|\varphi_n\rangle = \delta_{mn}$, it follows that $T^{(1)}_{mn}$ is a anti-Hermitian matrix, *i.e.*

$$T^{(1)}_{mn} = -T^{(1)*}_{nm} \tag{3.9}$$

Exercise: Derive this result by considering $\nabla\langle\varphi_m|\varphi_n\rangle$

Since electronic wave funtions can always be chosen real-valued, it means that diagonal effects of $T^{(1)}_{mn}$ vanish: $T^{(1)}_{nn}(\vec{R}) = 0$. Keeping only diagonal terms in equation (3.8) we obtain the adiabatic Schrödinger equation for the nuclei with an additional contribution from $T^{(2)}_{nn}$ which is usually small but non-vanishing

$$\left[\hat{T}_N + E_n(\vec{R}) + \hat{V}_N(\vec{R}) + T^{(2)}_{nn}(\vec{R})\right]\chi_n(\vec{R}) = E\chi_n(\vec{R}) \tag{3.10}$$

At avoided crossings, adiabatic states may change dramatically as a function of the nuclear coordinates. Derivatives with respect to nuclear displacements can therefore become large. In addition, non-adiabatic matrix elements as in equation (3.8) may be quite inconvenient to calculate.

In region of **avoided crossings**, a diabatic representation is more convenient.

[1] we neglect here the continuum which is, in principle, required

3.2.2 Diabatic representation

The alternative to the adiabatic basis is a diabatic basis which is chosen such that all electronic matrix elements of the derivatives $\frac{\partial}{\partial R}$ and $\frac{\partial^2}{\partial R^2}$ are as small as possible. There are infinitely many ways of choosing a diabatic basis. The simplest version consists in choosing the electronic basis functions to be independent of the nuclear geometry $\varphi(\vec{r};\vec{R}) \rightarrow \varphi(\vec{r};\vec{R}_0)$. This is called the "crude adiabatic" basis in which

$$\Psi(\vec{r};\vec{R}) = \sum_n \varphi_n(\vec{r};\vec{R}_0)\chi_n^{(0)}(\vec{R}). \tag{3.11}$$

The basis functions $\varphi_n(\vec{r};\vec{R}_0)$ are solutions of the electronic Schrödinger equation at geometry $\vec{R}_0$:

$$\hat{H}(\vec{r};\vec{R}_0)\varphi_n(\vec{r};\vec{R}_0) = \{\hat{T}_e + \hat{V}(\vec{r};\vec{R}_0)\}\varphi_n(\vec{r};\vec{R}_0) = E_n(\vec{R}_0)\varphi_n(\vec{r};\vec{R}_0) \tag{3.12}$$

where $\hat{V}(\vec{r};\vec{R}_0)$ includes $\hat{V}_e$, $\hat{V}_N$,$\hat{V}_{eN}$. Substituting equation (3.11) into equation (3.2), multiplying from the left with $\varphi_m(\vec{r},\vec{R}_0)$ and integrating over the electronic degrees of freedom we obtain

$$\sum_n \{\hat{T}_{nn}\delta_{nm} + U_{mn}\}\chi_n^{(0)} = E\chi_m^{(0)}, \tag{3.13}$$

where $U_{mn} = \langle\varphi_m(\vec{R}_0)|\hat{V}(\vec{r},\vec{R}) - \hat{V}(\vec{r},\vec{R}_0)|\varphi_n(\vec{R}_0)\rangle$ (Again, brackets imply integration over the electronic coordinates only).

Note the simplicity of equation (3.13) compared to equation (3.8). The transformation from the adiabatic into the diabatic basis has also transformed derivative couplings $(\frac{\mathrm{d}}{\mathrm{d}R})_{mn}$ into coordinate couplings $(\hat{U}(R))_{mn}$. Diagonal elements of U are diabatic surfaces and off-diagonal elements are non-adiabatic couplings which can cause non-adiabatic transitions. Equation (3.13) can be solved numerically by so-called "close-coupling methods". The crude adiabatic basis required for converging calculations of relevant molecular systems is often very large. In practice one looks for a conventional "diabatization scheme" that minimizes the coupling. The complete elimination of couplings in only possible for **diatomics**. The situation for **polyatomics** is generally more complicated and some non-adiabatic coupling remain. (For application see exercises).

3.3 Intersections of adiabatic potential energy surface

Particularly interesting is the case of **conical intersections**. We examine the intersection of adiabatic surfaces. In diatomics, adiabatic curves belonging to electronic states of the same symmetry generally do not cross but exhibit avoided crossings. The proof of this non-crossing rule is simple in a diabatic basis:

$$U_{mol} = \begin{pmatrix} U_{11} & U_{12} \\ U_{21} & U_{22} \end{pmatrix}.$$

The off-diagonal elements are zero, unless the states 1 and 2 have the same electronic symmetry. Diagonalization gives the adiabatic potentials

$$V_{\pm} = \frac{U_{11} + U_{22}}{2} \pm \frac{1}{2}\sqrt{(U_{11} - U_{22})^2 + 4|U_{12}|^2}. \tag{3.14}$$

The energy gap between the curves is

$$\Delta V = V_+ - V_- = \sqrt{(U_{11} - U_{22})^2 + 4|U_{12}|^2} \tag{3.15}$$

Curves only cross if $U_{11}(R) = U_{22}(R)$ and $U_{12}(R) = 0$ which represent two conditions to be met for one variable R. This is not possible in general in one dimension, leading to the non-crossing rule for diatomics. In two dimensions there is generally a single (or a discrete set of) points where the two surfaces touch leading to so-called conical intersections.

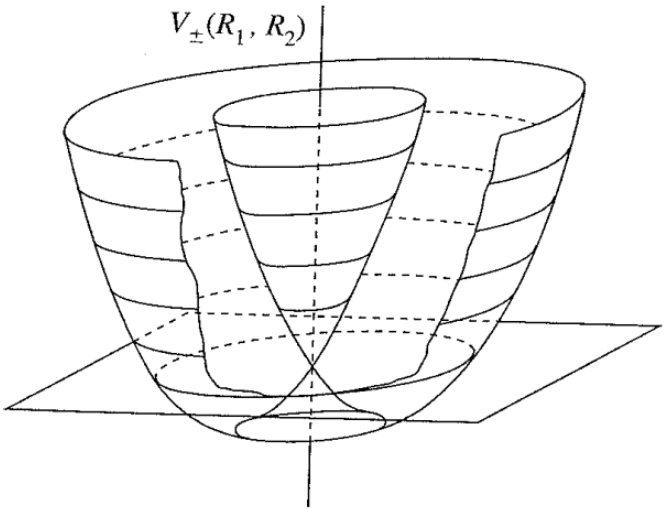

Figure 3.2: Potential energy functions $V_{\pm}$ as a function of two nonsymmetric nuclear coordinates showing the geometry of a conical intersection.(taken from Introduction to quantum mechanics, David J. Tannor)

In $n > 2$ dimensions, the intersection space is normally a manifold of dimension n-2 resulting from the two constraints given above e.g. triatomics $\rightarrow$ $3N$-6=3 $\rightarrow$ one-dimensional "seam" of conical intersections.

1. Conical intersections are essential in excited-state dynamics and cause rapid **internal conversion**, see e.g. Fig. 3.3.

2. Conical intersections also occur in all Jahn-Teller systems where they are enforced by symmetry.

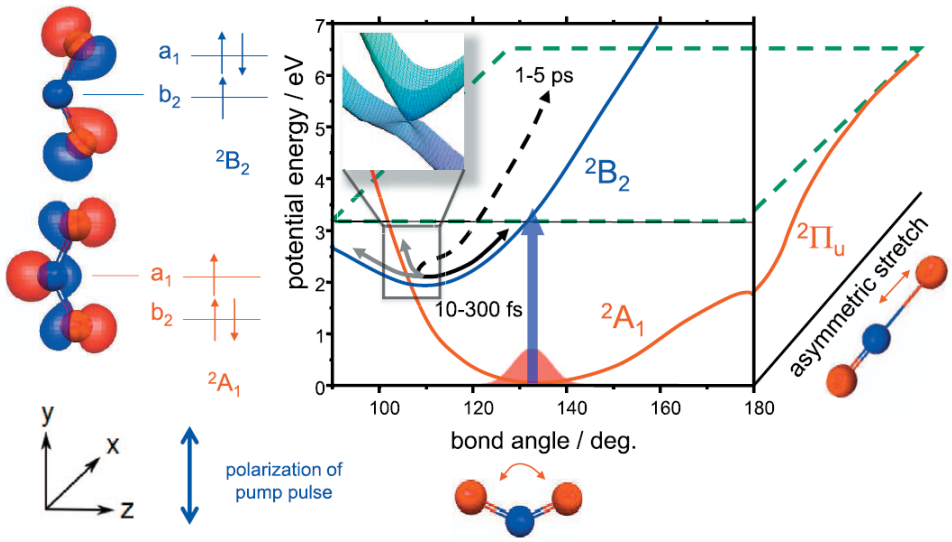

Figure 3.3: Potential energy surfaces of the ground ($\tilde{X}^2A_1$) and the first excited electronic state ($\tilde{A}^2B_2$) of NO_2. The left-hand panel shows the dominant electronic configuration in the two highest lying molecular orbitals. Taken from Science 334, 208 (2011)

3.4 Predissociation

Molecules in excited states can decay through a number of processes that can be classified into radiative and non-radiative transitions. The competition between radiative and non-radiative (e.g. dissociative) processes can be described kinetically

$$\begin{aligned} \mathrm{AB}^* &\rightarrow \mathrm{AB} + h\nu \\ \mathrm{AB}^* &\rightarrow \mathrm{A} + \mathrm{B} \\ \mathrm{d}N = -k_r N \mathrm{d}t - k_{nr} N \mathrm{d}t &\rightarrow N(t) = N_0 e^{-(k_r + k_{nr})t} = N_0 e^{-(\frac{t}{\tau})}, \end{aligned} \tag{3.16}$$

where $\frac{1}{\tau} = k_r + k_{nr} = \frac{1}{\tau_r} + \frac{1}{\tau_{nr}}$.

As a first example, we consider predissociation. A vibrational level lying **above** the lowest dissociation limit can dissociate. The mixing of a bound state $\psi_{1,v}$ and a continuum $\psi_{2,E}$ is governed by the interaction matrix elements

$$\begin{aligned} H_{V,E} &= \langle \psi_{1,v} | \hat{H} | \psi_{2,E} \rangle \\ &= \langle \phi_1(r,R)\chi_v(R) | \hat{H} | \phi_2(r,R)\chi_E(R) \rangle \end{aligned} \tag{3.17}$$

The discrete-state amplitude $a(E)$ in the continuum eigenfunction

$$\psi_E = a(E)\psi_{1,v} + \int dE' b_{E'}(E)\psi_{2,E'} \tag{3.18}$$

is given by

$$a(E) = \frac{H_{v,E}}{E - E_r + i\pi|H_{v,E}|^2} \tag{3.19}$$

When $H_{V,E}$ varies slowly with energy, $a(E)$ is a Lorentzian function with FWHM:

$$\Gamma_V = 2\pi|H_{V,E}|^2. \tag{3.20}$$

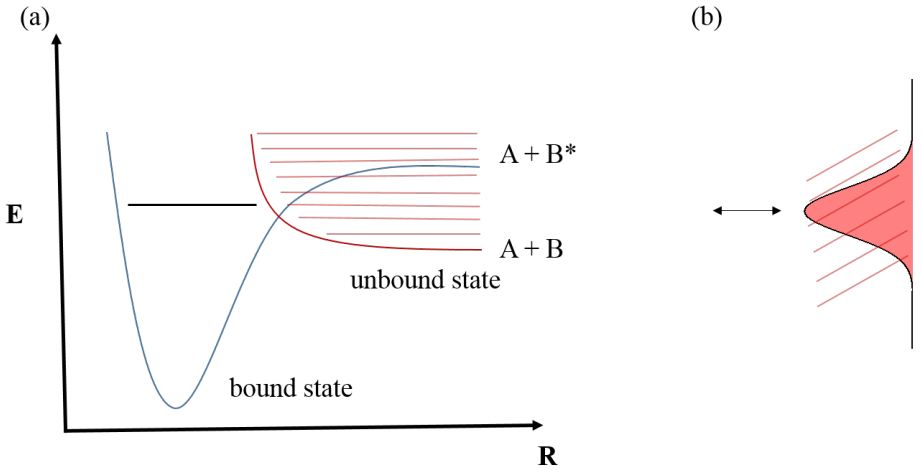

Figure 3.4: Illustration of predissociation caused by the crossing between the diabatic potential-energy curves of a bound and a repulsive state.

One also finds

$$\Gamma_V = 2\pi\rho(E)|H_{V,E}|^2 \tag{3.21}$$

which is **Fermi's golden rule** where $\rho(E)$ is the density of states.

The first expression (Eq. (3.20)) applies to **energy-normalized** states. The second (Eq. (3.21)) to **space-normalized** states. From here it is easy to show that the decay of the initially populated level is exponential in time:

$$\begin{aligned} A(t) = \langle\psi_{1,v}|\psi(t)\rangle &= \int_{-\infty}^{\infty} \mathrm{d}E \mathrm{e}^{[-\frac{\mathrm{i}}{\hbar}Et]}|a(E)|^2 \\ A(t) &\propto \mathrm{e}^{(-\frac{\Gamma t}{2\hbar})}\mathrm{e}^{(-\frac{\mathrm{i}E_r t}{\hbar})} \\ |A(t)|^2 &\propto \mathrm{e}^{-\frac{\Gamma t}{\hbar}} \end{aligned} \tag{3.22}$$

Example of predissociation caused by curve crossing: Schumann-Runge bands of O_2, λ <200 nm, shown in Fig. 3.5.

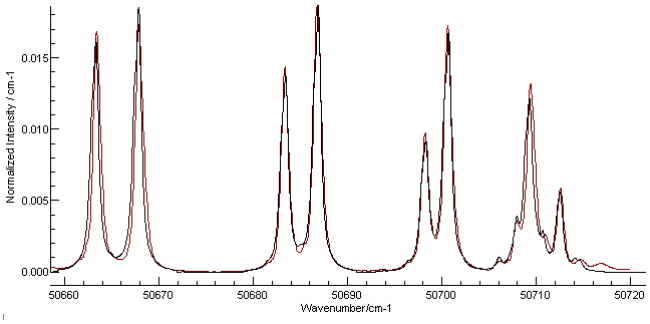

Figure 3.5: The absorption spectrum (red line) shows the 2-0 band of the B $^3\Sigma_u^-$-X $^3\Sigma_g^-$ system of O_2. Note the clear Lorentzian shape of the lines, caused by predissociation. Taken from `http://pgopher.chm.bris.ac.uk/Help/makeo2.htm` which also explains the simulation shown as black line.

A different type of predissociation occurs, when the rotational excitation of a molecule is sufficiently high that the centrifugal force leads to bond breaking. This situation is illustrated in Fig. 3.6, which shows both the adiabatic potential $V(R)$ of a diatomic molecule in its rotational ground state (usually $J = 0$) and the total potential given by the sum of $V(R)$ and the centrifugal potential $\frac{\hbar^2 J(J+1)}{2\mu R^2}$, where J is the rotational quantum number, μ is the reduced mass and R is the internuclear separation.

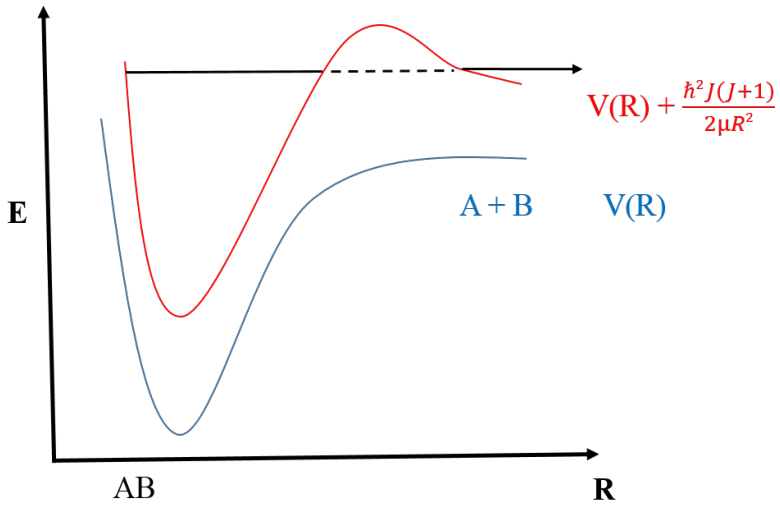

Figure 3.6: Illustration of rotational predissociation. The blue curve shows the adiabatic potential in the absence of rotational excitation ($J = 0$). The red curve is the total potential obtained by adding the centrifugal term, depending on the rotational quantum number J to the adiabatic potential.

Example of rotational predissociation: Electronic spectrum of Se_2, shown in Fig.

3.7.

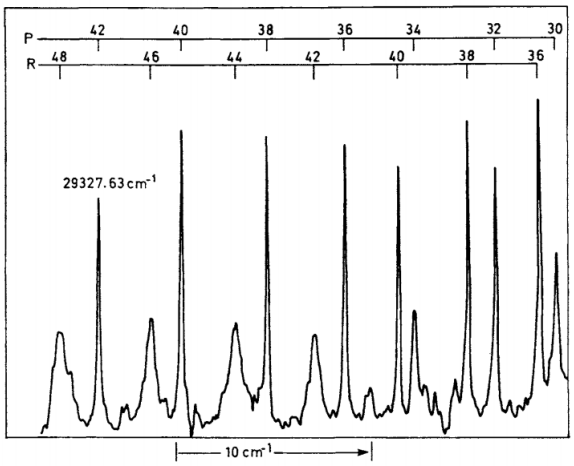

Figure 3.7: The absorption spectrum shows the 15-0 band of the B 0_u^+-X 0_g^+ system of $^{78}Se_2$. The linewidths increase with the rotational quantum number J' in the electronically-excited B state, which is given on the assignment bar above the spectrum. Taken from The Spectra and Dynamics of Diatomic Molecules, H.Lefebvre-Brion and Robert W. Field.

3.5 Fano lineshapes

Lineshapes in spectral regions where predissociation or autoionization occur are often asymmetric instead of having a Lorentzian shape. These so-called Fano lineshapes (see figure 3.8) arise from interference between bound-bound and bound-continuum transitions on opposite sides of the line center.

The corresponding absorption cross section has the form

$$\begin{aligned} \sigma_a(\epsilon) &= \sigma_i \frac{(q+\epsilon)^2}{1+\epsilon^2} \\ \text{where } \epsilon(E) &= \frac{E-E_r}{\Gamma/2} \end{aligned} \tag{3.23}$$

is the dimensionless energy offset from the line center and σ_i is the "non-resonant" bound-continuum cross section. The parameter q defines the shape of the absorption line with $q = 0$ corresponding to a symmetric "window resonance", $q \to \infty$ to a Lorentzian line, $q < 0$ asymmetric line shapes with a maximum preceding a minimum and vice-versa for $q > 0$. The Fano q-parameter is defined as follows:
The bound and continuum basis functions of the upper level within the Born-Oppenheimer approximation are $\phi_1\chi_v$ and $\phi_2\chi_E$ respectively. The true eigenstate is then given as a function of energy by:

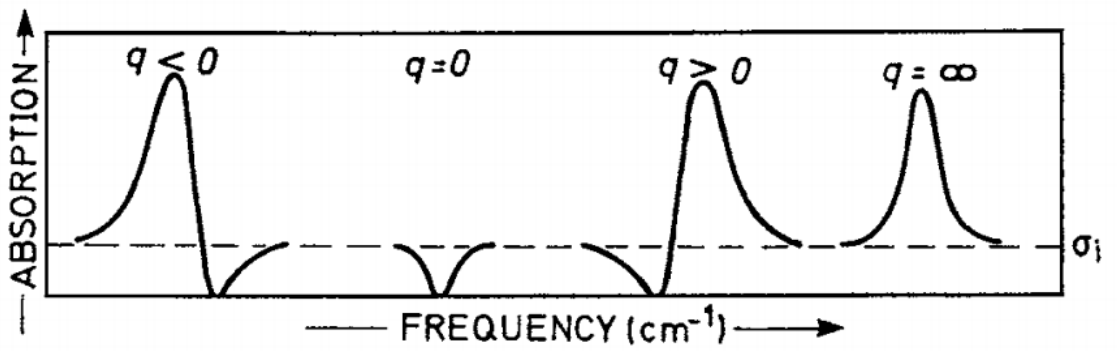

Figure 3.8: Fano profiles for q <0, q =0, q >0 and $q \to \infty$ and $(-\infty)$. In the absence of a predissociated level the dotted line represents to the continuous background absorption (σ_i). Taken from The Spectra and Dynamics of Diatomic Molecules, H.Lefebvre-Brion and Robert W. Field.

$$\psi_E = a(E)\phi_1\chi_v + \int \mathrm{d}E' b_{E'}(E)\phi_2\chi_{E'} \tag{3.24}$$

and the transition moment from the ground state $\phi_0\chi_0$ to the final eigenstate is

$$\begin{aligned}\langle\psi_E|\vec{\mu}|\phi_0\chi_0\rangle = a^*(E)\,\langle\phi_1|\vec{\mu}|\phi_0\rangle\,\langle\chi_v|\chi_0\rangle \\ + \langle\phi_2|\vec{\mu}|\phi_0\rangle \int \mathrm{d}E' b^*_{E'}(E)\,\langle\chi_{E'}|\chi_0\rangle\end{aligned} \tag{3.25}$$

Ugo Fano, (Phys. Rev. 124, 1866 (1961)) showed that $|\,\langle\psi_E|\vec{\mu}|\phi_0\chi_0\rangle\,|^2$ has the form of equation (3.23) where

$$q_V \approx \frac{1}{\pi}\frac{\langle\phi_1|\vec{\mu}|\phi_0\rangle\langle\chi_v|\chi_0\rangle}{\langle\phi_2|\vec{\mu}|\phi_0\rangle\langle\chi_E|\chi_0\rangle}\frac{1}{\langle\phi_1|\hat{H}|\phi_2\rangle\langle\chi_v|\chi_E\rangle}. \tag{3.26}$$

3.6 Autoionization

An energy level lying above the lowest ionization limit can **autoionize**. In almost all molecules $E_{\mathrm{diss}} < E_{\mathrm{ion}}$ (famous exception is C_{60}) therefore several processes usually compete:

$$\mathrm{AB}^{**} \Rightarrow \begin{cases}\mathrm{AB}^+ + e^-, & \text{autoionization} \\ \mathrm{A} + \mathrm{B}^*, & \text{dissociation} \\ \mathrm{AB} + h\nu, & \text{radiative decay}\end{cases}$$

$$\Gamma = \Gamma_a + \Gamma_\mathrm{d} + \Gamma_r. \tag{3.27}$$

The autoionization width of an initial state $1, v$ into a final state $2, v^+$ of the cation with an electron of kinetic energy ϵ is

$$\Gamma_{1,n,v;2,\epsilon,v^+} = 2\pi |H_{1,n,v;2,\epsilon,v^+}|^2. \tag{3.28}$$

The same results as in the case of predissociation apply. Fano lineshapes are usually observed (see figure 3.9). In the time domain, autoionization leads to an exponential decay of the initially populated state.

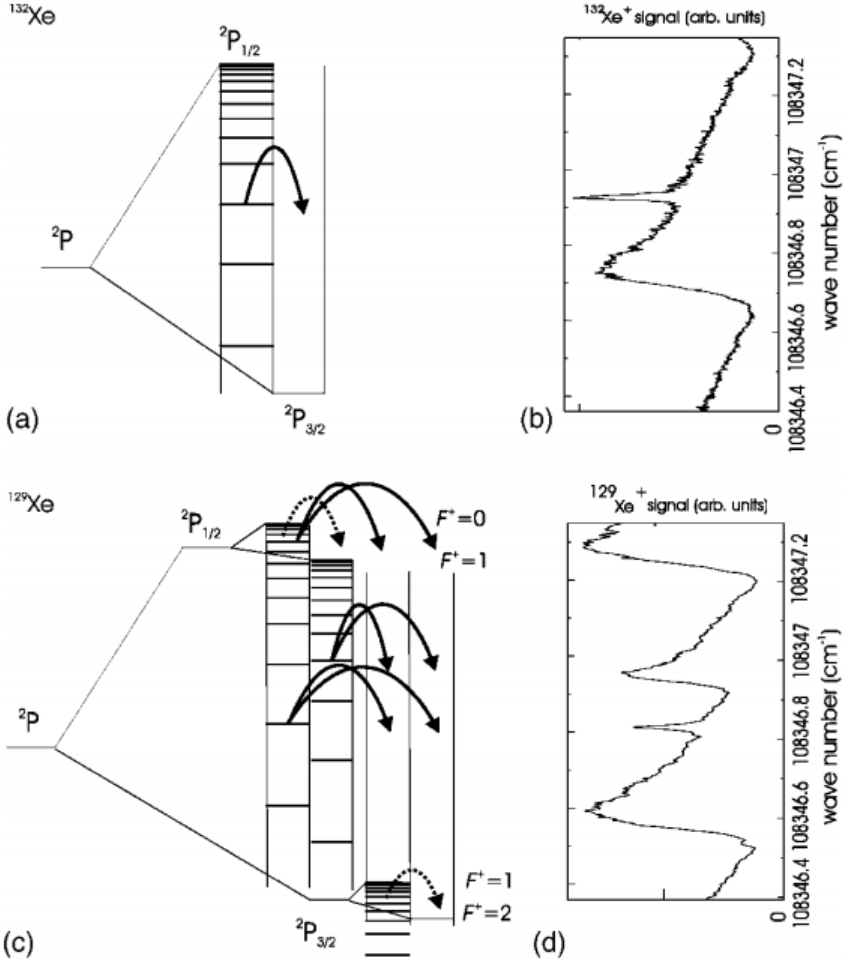

Figure 3.9: Schematic energy-level diagram of the autoionizing Rydberg series of ^{132}Xe (a) and ^{129}Xe (c). Spin-orbit autoionization is represented by full arrows and dotted arrows in panel (c) represent the hyperfine autoionization process. Photoionization spectra of ^{132}Xe and ^{129}Xe are shown in (b) and (d), respectively. Taken from *Phys. Rev. A* 71, 052504 (2005).

3.7 Light-matter interaction

- An electromagnetic field can be represented as a collection of modes occupied with n quanta (similar to the harmonic oscillator).
- Coherent radiation corresponds to very high numbers of quanta per mode, typical numbers are $10^{10} - 10^{20}$.
- Coherent light with high occupation numbers can be treated classically (using Maxwell's equations).
- This is not the case for thermal light sources which require a quantum-statistical description.

Dipole approximation: for $\lambda >> d$ (extension of atom/molecule) we obtain:

$$\begin{aligned} \hat{V}_{el}(t) &= -\underbrace{\left(\sum_i \hat{q}_i \vec{r}_i\right)}_{=\vec{\mu}_{el}} \cdot \vec{E}_0^{(z)} \cos(\omega t + \phi) \\ \text{Similarly: } \hat{V}_{mag}(t) &= -\vec{\mu}_{mag}.\vec{B}_0^{(x)} \cos(\omega t + \phi) \end{aligned} \tag{3.29}$$

Optical domain: $\hat{V}_{el}$ dominates in the optical domain but EPR and NMR rely on $\hat{V}_{\text{mag}}$. TDSE in dipole approximation can be written:

$$\mathrm{i}\hbar\frac{\partial\psi}{\partial t} = (\hat{H}_{mol} - \vec{\mu}\cdot\vec{E}_0^{(z)}\cos(\omega t+\phi))\psi \tag{3.30}$$

As usual we write the solution in eigenstates of the field-free Hamiltonian:

$$\begin{aligned} \psi(t) &= \sum b_k(t)\phi_k(\vec{r},\vec{R}) \\ \text{i.e. } \mathrm{i}\hbar\frac{\partial}{\partial t}\sum_k b_k\phi_k &= \hat{H}\sum_k b_k\phi_k \\ \text{therefore } \mathrm{i}\hbar\frac{\mathrm{d}b_j(t)}{\mathrm{d}t} &= \sum_k H_{jk}b_k(t) \\ \mathrm{i}\hbar\frac{\mathrm{d}}{\mathrm{d}t}\vec{b}(t) &= \mathbf{H}\vec{b}(t) \end{aligned} \tag{3.31}$$

3.7.1 Rabi oscillations in two-level system

We consider a two-level system:

This two-level system is assumed to be described by a field-free Hamiltonian $\hat{H}_{\text{mol}}$ and a time-dependent interaction $\hat{V}(t)$ with an electromagnetic field:

$$\mathbf{H}_{mol} = \begin{pmatrix} E_1 & 0 \\ 0 & E_2 \end{pmatrix} = \begin{pmatrix} \hbar\omega_1 & 0 \\ 0 & \hbar\omega_2 \end{pmatrix}$$

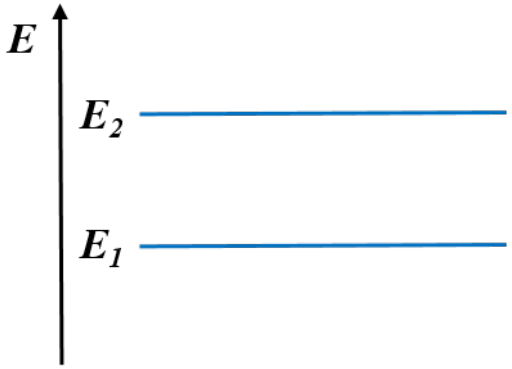

$$\mathbf{V}(t) = \begin{pmatrix} 0 & \hbar V_{12}\cos(\omega t + \phi) \\ \hbar V_{21}\cos(\omega t + \phi) & 0 \end{pmatrix}$$

where $V_{12} = -\frac{\langle\phi_1|\hat{\mu}_z|\phi_2\rangle E_0^{(z)}}{\hbar} = V_{21}^*$.
For ϕ_1 and ϕ_2 real, $V_{12} = V_{21} = V$ is also real.
We obtain

$$\begin{aligned} \mathrm{i}\frac{\mathrm{d}b_1}{\mathrm{d}t} &= \omega_1 b_1 + V_{12}\cos(\omega t + \phi) b_2 \\ \mathrm{i}\frac{\mathrm{d}b_2}{\mathrm{d}t} &= V_{21}\cos(\omega t + \phi) b_1 + \omega_2 b_2 \end{aligned} \tag{3.32}$$

Only approximate solutions of this system of coupled differential equations are known analytically. Close to resonance with detuning

$$\Delta = (\omega_2 - \omega_1) - \omega = \omega_{12} - \omega \tag{3.33}$$

The following approximate solution is known:

$$p_2(t) = |b_2(t)|^2 = \frac{V^2}{V^2 + \Delta^2}\left(\sin(\frac{t}{2}\sqrt{V^2 + \Delta^2})\right)^2 = 1 - p_1(t) \tag{3.34}$$

which is a periodic function with period $T = \frac{2\pi}{\sqrt{V^2+\Delta^2}}$.